Development of High Performance Aircraft Bleed Air Temperature Control System With Reduced Ram Air Usage

Lan Shang, Guangjun Liu, *Senior Member, IEEE*, and Peter Hodal

***Abstract*—Conventional aircraft engine bleed air temperature regulation system is inefficient due to unnecessary ram air usage in cooling the bleed air, which in turn causes unnecessary drag and fuel consumption. This paper proposes an aircraft bleed air temperature control system, aiming at minimizing the ram air usage to reduce drag and fuel consumption while maintaining fast temperature control response. To achieve both of the objectives, a new control system configuration is developed to control both ram air and bypass flows in such a way that the bypass bleed air flow is automatically controlled at a small level that is just sufficient to maintain fast regulation of the flow temperature at the load. Analytical equations describing the system dynamics and linearized model are derived and utilized in the overall bleed air temperature control design and analysis. PI control and optimal output feedback are investigated. Computer simulations and experiments have been conducted, and the proposed control system is shown to be effective in reducing ram air usage and maintaining fast temperature control response in the meantime.**

***Index Terms*—Aircraft, bleed air, optimal control, ram air, temperature control.**

I. Introduction

BLEED air in gas turbine engines is compressed air taken from within the engine. This high-pressure and high-temperature engine bleed air is commonly used for various tasks on the aircraft, including deicing, pressurizing the cabin, and air conditioning for passengers and avionics equipment [1]–[4]. Some of the tasks require that the supply bleed air be regulated at a certain temperature for its efficient use. It is critical to control the temperature of the supply air with fast transient response and adequate steady-state accuracy.

Ram air is commonly used to cool the engine bleed air, and it is scooped from the aircraft boundary layer or close to it. The external air is forced through a scoop, which faces into the external air flow, a heat exchanger matrix and then rejected overboard by forward motion of the aircraft. A large ram air usage increases the aircraft drag and weight because of the resistance of the scoop, pipe work, and the heat exchanger matrix.

Thermal conditioning of the hot engine bleed air is accomplished by first passing it through a heat exchanger device. Compact (crossflow) heat exchangers are commonly used, due to their low weight and space requirement, and a high heat transfer area [5]. The heat energy from the bleed air is transferred to the ram air stream.

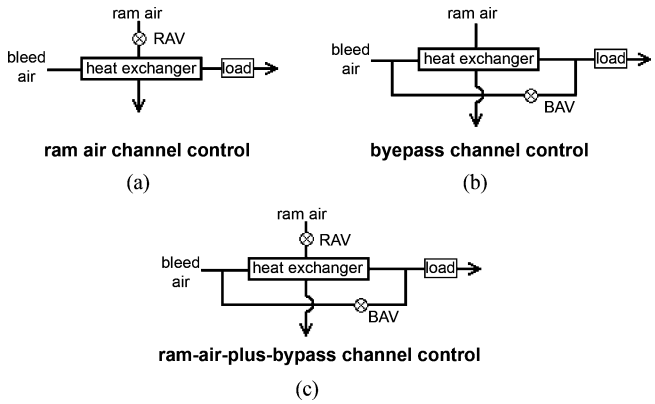

Fig. 1. Three control configurations.

The occurrence of heat exchange between the bleed air and ram air streams is of vital importance in the bleed air system. Various works have been done to improve the performance of the heat exchanger based temperature regulation systems. While sharing many common characteristics, they differ mainly in the control valve configuration and the applied control law [6]–[9]. As addressed in [9], it is common that control is achieved without changing the total stream flow rates. In the engine bleed air temperature regulation system, overall flow rate is set by the operating conditions. The air temperature at the load is regulated by either changing the ram air flow rate, or the bleed air main/bypass flow ratio, or a combination of both.

Two known control system configurations as shown in Fig. 1(a) and (b) and one proposed as shown in Fig. 1(c) are analyzed and compared in this paper. In the first configuration, Fig. 1(a), a control valve (*RAV*) is placed into the ram air channel. The valve manipulates the flow rate of the ram air, thus affecting the temperature of the bleed air stream leaving the heat exchanger, which is equal to the air temperature at the load. The second control strategy, Fig. 1(b), is termed bypass channel control. In this configuration, most of the bleed air goes through the hot-side of the heat exchanger, while a small portion of the overall bleed-flow is made to bypass the heat exchanger via the bypass channel, to be mixed downstream with the main bleed air flow leaving the heat exchanger. The combined air flow then proceeds to the load. A control valve (*BPV*) is located in the bypass channel to manipulate the ratio of main-to-bypass bleed air flows, thus regulating the temperature of the flow delivered to the load.

The first configuration [see Fig. 1(a)] uses only sufficient ram air to cool the bleed air down to the required temperature, but its temperature control response is slow due to the heat exchanger

Manuscript received April 14, 2008. Manuscript received in final form April 20, 2009. First published July 28, 2009; current version published February 24, 2010. Recommended by Associate Editor R. E. Young. This work was supported in part by the Natural Sciences and Engineering Research Council (NSERC) of Canada and by the Canada Research Chair Program.

L. Shang and G. Liu are with the Department of Aerospace Engineering, Ryerson University, Toronto, ON M5B 2K3 Canada (e-mail: gjliu@ryerson.ca).

P. Hodal is with Honeywell Engines & Systems, Mississauga, ON L5L 3S6 Canada.

Color versions of one or more of the figures in this paper are available online at http://ieeexplore.ieee.org.

Digital Object Identifier 10.1109/TCST.2009.2021647

dynamics. The second configuration [see Fig. 1(b)] can regulate the bleed air temperature at the load with fast transient response, but it requires excessive ram air usage and causes unnecessary fuel consumption. The proposed configuration as shown in Fig. 1(c) is termed ram-air-plus-bypass channel control, which essentially combines aspects of both former arrangements, aiming to reduce ram air usage and to maintain efficient load temperature control. A control valve is placed in the ram air channel as well as in the bypass channel, and the ram air and bypass flows are controlled in such a way that the bypass bleed air flow is automatically controlled at a level that is just sufficient to maintain fast temperature regulation of the bleed air flow.

Conventional PI control and linear quadratic (LQ) control techniques are applied for the bypass channel valve and ram air channel valve control for the proposed system configuration. LQ optimal control has been applied in a broad range of temperature control systems and other applications. Forrest *et al.* [10] implemented a primary LQ controller in their study of super-heater steam control, proposing periodic plant sampling and controller self-tuning for their outer loop controller. Katayama *et al.* [6] investigated an optimal tracking control of a heat exchanger with load change, and derive an optimal tracking controller with integral, state feedback plus preview actions. Orzylowski *et al.* [11] discussed optimal and suboptimal control, based on the linear quadratic performance index, for their furnace batch temperature control system. Pederson *et al.* [12] applied LQ control to a power plant boiler.

In this paper, in order to control the valves in the ram-air-plus-bypass channel configuration as shown in Fig. 1(c) to minimize the ram air usage while maintaining fast temperature control response, the analytical equations describing the system dynamics are derived, based on which a LQ regulator (LQR) is designed. Both the temperature control error and the bypass channel valve opening deviation from its set point are taken into account in the quadratic performance index function to be optimized. In such a way the bypass air flow is automatically controlled at a low level that is just sufficient to maintain fast temperature regulation of the bleed air flow, and only necessary ram air is used to maintain the temperature at the load. Computer simulations and experiments have been conducted for all the configurations in Fig. 1 at a selected operating point with consideration of disturbances, and the proposed control system is shown to be more effective in minimizing ram air usage and maintaining fast temperature control response in the meantime.

The rest of this paper is presented in the following manner. The system model is formulated in Section II. The control system design and analysis are presented in Section III. In Section IV, simulations are presented along with discussions and comparisons. Experiments are conducted to further investigate the effectiveness of the proposed ram-air-plus-bypass control strategy, and the results are presented in Section V. Finally, conclusions are drawn based on the simulation and experimental results in Section VI.

II. System Model

A. System Configuration and Modeling Assumptions

As shown in Fig. 2, the hot bleed air comes from aircraft engine, at a temperature of $T_{hi}(^\circ\mathrm{F})$, pressure P_{hin} (psi), and a mass flow rate W_{bleed} (lb/s). Ram air is from the atmosphere at a mass flow rate W_{ram} (lb/s). Inlet pressure P_{cin} (psi) and temperature $T_{cin}(^\circ\mathrm{F})$ are determined from the ambient temperature $T_{amb}(^\circ\mathrm{F})$ and ambient pressure P_{amb} (psi)

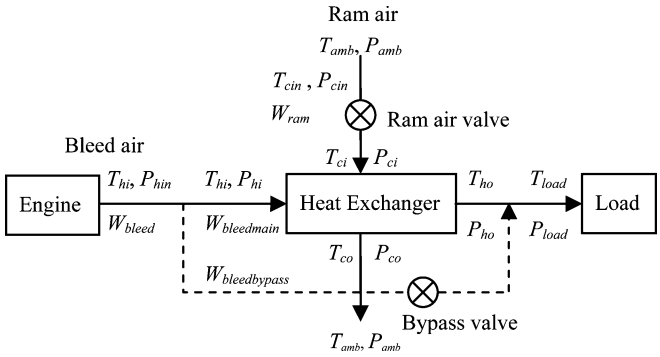

Fig. 2. Schematic diagram of the proposed system configuration.

$$T_{cin} = (T_{amb} + 460)\left(1 + 0.2\mathrm{Mach}^2\right) - 460 \tag{1}$$

$$P_{cin} = F_{rec}\left(P_{amb}\left(1 + 0.2\mathrm{Mach}^2\right)^{3.5} - P_{amb}\right) + P_{amb} \tag{2}$$

where F_{rec} is the pressure recovery factor, and Mach is the Mach number.

For configurations with a bleed air bypass, the hot bleed air is divided into two channels, namely the main bleed air and bypass channel, which are at mass flow rates $W_{bleedmain}$ (lb/s) and $W_{bleedbypass}$ (lb/s), respectively. The main bleed air is cooled by ram air through the heat exchanger and mixed with bypass flow downstream.

Control valves are placed in the ram air channel and/or the bypass channel which can be controlled to regulate the load temperature. To simplify the system, some assumptions are made as follows [13]:

a) transport delay between components is negligible;
b) there is no heat loss from the pipes to surrounding air;
c) pressure loss due to pipe flow is negligible; and the flow is assumed to be fully developed.

B. Heat Exchanger

The heat exchanger core is modeled by a thin plate surface (2-D) which separates the hot and cold air streams as illustrated in Fig. 3. A pure cross-flow configuration is considered, with both fluids unmixed as they pass over the plate on their respective sides. The hot side fluid (bleed air) with a specific heat of C_h (Btu/lb $\cdot^\circ$ F) flows at a flow rate $W_{bleedmain}$, and with the inlet temperature of T_{hi} and outlet temperature of $T_{ho}(^\circ\mathrm{F})$. The cold side fluid (ram air) with a specific heat of C_c flows at W_{ram}, and with inlet and outlet temperatures $T_{ci}(^\circ\mathrm{F})$ and $T_{co}(^\circ\mathrm{F})$, respectively. The heat exchanger core has a thermal mass of MC_s (Btu/$^\circ$F) and a surface temperature of T_s.

For an ideal gas with constant specific heat capacity C, the change of fluid temperature is [14]

$$dT = -\frac{dq}{WC} \tag{3}$$

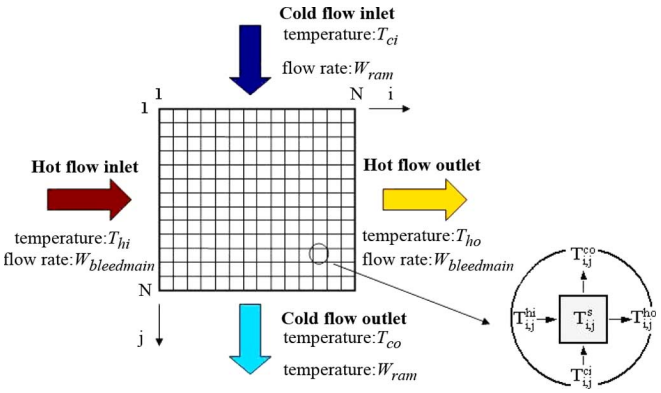

Fig. 3. Partitioning of the heat exchanger plate.

where W is the fluid flow rate (lb/s), dt is the incremental temperature (°F), and dq is the incremental heat transfer (Btu/s) which follows from Newton's law of cooling

$$dq = h(T - T_s)dx \tag{4}$$

where h (Btu/s·° R · ft) is the heat transfer coefficient (per unit depth), and dx is the incremental length.

Equating the heat lost by the fluid to the heat transferred to the surface, and integrating along the length L of the surface, leads to the following equation of the total heat transferred to the surface

$$q = WC\left(1 - e^{-H/WC}\right)(T_i - T_s) \tag{5}$$

where T_i is the fluid inlet temperature, and $H = hL$ (Btu/s·°R) is the total heat transfer coefficient (per unit depth) between the fluid and the surface.

For this study, the overall heat transfer coefficients are given as experimentally-determined functions of flow rate, with H_h and H_c denoting the hot and cold side coefficients, respectively. The hot and cold side inlet pressures are denoted by P_{hi} (psig) and P_{ci} (psig), respectively, and P_{ho} (psig) and P_{co} (psig) denote the hot and cold side outlet pressures.

The lump surface temperatures T_s are selected to form the state space vector (assumed uniformly distributed throughout each lump). The hot and cold fluid temperatures follow from the surface temperatures using the appropriate algebraic equations, in the form of (5). Note that this equation is valid for constant surface temperature only; however, by using an infinitesimal time step dt, one can approximate that the surface temperature is not changing during that time slice.

The dynamics of the heat transfer to the cell core are governed by the following differential equation:

$$\frac{d(MC_sT_s)}{dt} = q_h + q_c \tag{6}$$

where q_h and q_c represent heat transfer to the surface from the hot and cold sides, respectively, which follow from (5), with the appropriate substitutions made with respect to hot and cold side variables.

The heat transfer surface is split up into $N \times N$ equal area lumps, where the dimension N is user specified. The state (6) can now be rewritten on a "per cell" basis, using indices to indicate the exact cell

$$\dot{T}^s_{i,j} = \psi T^s_{i,j} + \theta T^{hi}_{i,j} + \varphi T^{ci}_{i,j} \tag{7}$$

where

$$\psi = \frac{-W_{bleedmain}C_h a - W_{ram}C_c b}{MC_s}$$
$$\theta = \frac{W_{bleedmain}C_h a}{MC_s}$$

and

$$\varphi = \frac{W_{ram}C_c b}{MC_s}$$
$$a = 1 - e^{-H_h/W_{bleedmain}C_h}$$
$$b = 1 - e^{-H_c/W_{ram}C_c}$$

$i = 1, 2, \ldots, N;\ j = 1, 2, \ldots, N.$

Two algebraic equations representing the convection heat transfer relate the hot/cold cell output temperatures to the cell core temperature and cell inlet temperatures

$$T^{ho}_{i,j} = (1 - a)T^{hi}_{i,j} + aT^s_{i,j} \tag{8a}$$
$$T^{co}_{i,j} = (1 - b)T^{ci}_{i,j} + bT^s_{i,j}. \tag{8b}$$

By geometry, lump inlet temperatures are related to the outlet temperatures of adjacent lumps

$$T^{hi}_{i,j} = T^{ho}_{i-1,j} \quad T^{ci}_{i,j} = T^{co}_{i,j-1}. \tag{9}$$

C. Control Valve and Flow Rate

Neglecting valve hysteresis and backlash, the valve dynamics are modeled as a first-order lag

$$\beta_v(s) = u_v(s)\frac{K_v}{\tau_v s + 1} \tag{10}$$

where u_v is the opening-command input to the valve (0%-100%), β_v is the valve opening angle (rad), K_v is the valve gain, and τ_v is the valve time constant. The corresponding valve opening area A_v is then calculated

$$A_v = \frac{\pi D_v^2}{4}(1 - \cos\beta_v) \tag{11}$$

where D_v is the valve diameter.

The air flow rate W_v (lb/s) passing a valve is calculated using an equation for isentropic expansion process for variable area duct flow

$$W_v = \frac{A_v P_u}{\sqrt{T_u}}\left[\frac{2\gamma g}{(\gamma - 1)R}\left(\phi^{2/\gamma} - \phi^{(1+\gamma)/\gamma}\right)\right]^{1/2}$$
$$\phi = \frac{P_d}{P_u} \tag{12}$$

where P_u and P_d are the upstream and downstream pressures (psi), respectively, T_u is the upstream temperature (°R), $g = 32.174$ ft/s^2 is the acceleration of gravity, $R = 1717$ ft^2/(s^2 ·° R) is the gas constant for air, and $\gamma = 1.4$ (for air) is the ratio of specific heat at constant pressure to specific heat at constant volume. In ram air channel, the following equations hold: $W_v = W_{ram}$, $P_u = P_{cin}$, $P_d = P_{ci}$, and $T_u = T_{ci}$; and for the bypass

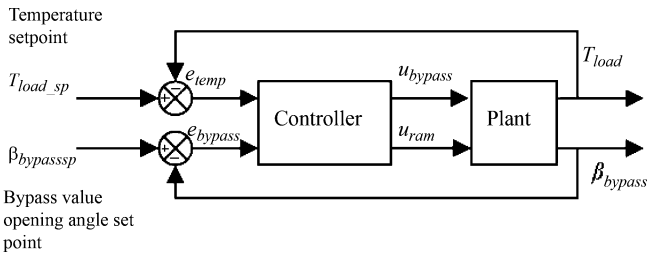

Fig. 4. Ram-air-plus-bypass control strategy.

channel, $W_v = W_{bleedbypass}$, $P_u = P_{hin}$, $P_d = P_{load}$ (load pressure), and $T_u = T_{hi}$.

D. Load Temperature and Pressure

For configurations with a bypass, the bypass channel flow merges back with the main bleed flow before the joined stream is delivered to the load. Assuming perfectly mixed flow, the load temperature $T_{load}(^\circ\mathrm{F})$ is then given by

$$T_{load} = \frac{T_{ho}W_{bleedmain} + T_{hi}W_{bleedbypass}}{W_{bleed}}. \tag{13}$$

For the control strategies studied in this paper, the load is simplified by an impedance equation with a suitable pressure drop

$$P_{load} = KW_{bleed}^2 + P_{amb} \tag{14}$$

where K is the load impedance constant.

III. Control Design

The key in the control system design for the proposed ram-air-plus-bypass channel configuration is to properly control the bypass channel such that both fast temperature response and reduction of ram air usage are achieved. To reach this goal, a small bypass valve opening is selected as a set-point, which is to be maintained at steady state. Upon system transient and disturbances, the bypass valve opening is controlled to provide a fast response in regulating the load temperature. However, since a reduction in ram air usage is sought along with fast transient, it is desired to have a low bypass flow rate. By setting the bypass valve set-point to a value that will result in a fairly low (e.g., 10%) bypass ratio (bypass flow rate to total bleed flow rate), it is ensured that the system is not overcooled to a large extent, which results in unnecessary ram air usage and associated fuel consumption.

In the proposed control system architecture as shown in Fig. 4, the bypass channel valve opening ratio u_{bypass} and ram air valve opening ratio u_{ram} are treated as control inputs. The bypass channel valve will strive to bring about fast temperature regulation, while the ram air channel valve loop will act to let the bypass channel valve return to its predefined set-point.

This control strategy can be implemented using conventional PI control with two control loops. The bypass channel loop regulates the load temperature with the following PI control law

$$u_{bypass} = \left(K_{P_{bypass}} + \frac{K_{P_{bypass}}}{T_{I_{bypass}}S}\right) e_{temp} \tag{15}$$

where e_{temp} is the temperature error defined as the difference between the load temperature T_{load} and its set-point T_{load_sp}; $K_{Pbypass}$ and $T_{Ibypass}$ are the PI-controller proportional gain and integral time constant, respectively.

The ram air channel loop is driven by the bypass-valve opening error e_{bypass}, defined as the difference between the bypass valve opening and its predefined set-point, and the control law is given by

$$u_{ram} = \left(K_{P_{ram}} + \frac{K_{P_{ram}}}{T_{I_{ram}}S}\right) e_{bypass} \tag{16}$$

where K_{Pram} and T_{Iram} are the PI-controller proportional gain and integral time constant, respectively.

The ram-air controller action is indirect in nature and requires that the bypass control loop is closed; in this way, it forms the outer control loop, with the bypass controller being the inner control loop.

The above described PI control is simple, and similar controllers are commonly used in industry. However, the control system performance can be improved by using more advanced control techniques, such as optimal control.

In this work, LQR is also investigated in order to optimize the performance of the bleed air temperature regulation system, which is expected to be more efficient especially for aircraft in cruising flight. In order to implement LQR, the bleed air system model needs to be linearized at the nominal operating conditions and written in the state-space form

$$\Delta\dot{X} = A\Delta X + B\Delta U \tag{17}$$

$$\Delta Y = C\Delta X \tag{18}$$

in which ΔX, ΔU, and ΔY are the changes of state vector X, input vector U, and output vector Y, respectively, which are defined along with the system matrices A, B, and C in the following.

The state vector X consists of the heat exchanger core temperature vector $\hat{X}$, bypass valve opening angle β_{bypass}, ram air valve opening angle β_{ram}

$$X = [\,\hat{X}^T \quad \beta_{bypass} \quad \beta_{ram}\,]^T \tag{19}$$

in which the vector $\hat{X}$ consists of the heat exchanger cell temperatures as

$$\hat{X} = [T_{11}^s, \ldots, T_{1N}^s, T_{21}^s, \ldots, T_{N1}^s, \ldots, T_{NN}^s]^T. \tag{20}$$

The control input vector contains the commanded bypass channel valve opening ratio u_{bypass} and ram air valve opening ratio u_{ram}, and with the form

$$U = [\,u_{bypass} \quad u_{ram}\,]^T = [\,U_1 \quad U_2\,]^T. \tag{21}$$

There are totally $(N \times N + 2)$ state equations

$$\dot{X}_k = f_k(X, U), \quad k = 1, 2, \ldots, (N \times N + 2). \tag{22}$$

Equation (22) are linearized at the nominal operating conditions and written in the following form:

$$\begin{aligned}\Delta\dot{\hat{X}}_k = &\left.\frac{\partial f_k}{\partial \hat{X}_1}\right|_{\hat{X}_{1_o}} \Delta\hat{X}_1 + \left.\frac{\partial f_k}{\partial \hat{X}_2}\right|_{\hat{X}_{2_o}} \Delta\hat{X}_2 + \cdots \\ &+ \left.\frac{\partial f_k}{\partial \hat{X}_{N\times N}}\right|_{\hat{X}_{N\times N_o}} \Delta\hat{X}_{N\times N} \\ &+ \left.\frac{\partial f_k}{\partial \beta_{bypass}}\right|_{\beta_{bypass_o}} \Delta\beta_{bypass} + \left.\frac{\partial f_k}{\partial \beta_{ram}}\right|_{\beta_{ram_o}} \Delta\beta_{ram} \\ &+ \left.\frac{\partial f_k}{\partial U_1}\right|_{U_{1_o}} \Delta U_1 + \left.\frac{\partial f_k}{\partial U_2}\right|_{U_{2_o}} \Delta U_2 \\ &k = 1, \ldots, N\times N + 2. \quad (23)\end{aligned}$$

Rewriting (23) yields the matrices A and B, the elements of which are evaluated at the nominal operating conditions.

There are two outputs of interest: load temperature T_{load} and bypass valve opening angle β_{bypass}. Hence, the output vector Y is defined as

$$Y = [T_{load} \quad \beta_{bypass}]^T. \quad (24)$$

The associated output matrix C is with the dimension of 2 by $(N \times N + 2)$

$$C = \begin{bmatrix} \left.\frac{\partial T_{load}}{\partial \hat{X}_1}\right|_{\hat{X}_{1o}} & \cdots & \left.\frac{\partial T_{load}}{\partial \beta_{bypass}}\right|_{\beta_{bypass}} & \left.\frac{\partial T_{load}}{\partial \beta_{ram}}\right|_{\beta_{ram}} \\ 0 & \cdots & 1 & 0 \end{bmatrix}. \quad (25)$$

The output feedback optimal control law is defined as

$$\Delta U = -K_{lq}\Delta Y \quad (26)$$

where the gain K_{lq} is determined by minimizing the quadratic performance index

$$J = \frac{1}{2}\int_0^\infty \left(\Delta X^T Q \Delta X + \Delta U^T R \Delta U\right) dt \quad (27)$$

where Q and R are the "penalty" weighting matrices.

IV. Simulation Results

Using the dynamic equations and control laws derived in the previous sections, simulation studies have been conducted for all three control configurations shown in Fig. 1. Disturbances arising from changes in engine loading and/or atmospheric conditions are considered. The simulation results for a $40\,^\circ$F step increase in bleed air temperature T_{hi} are presented here. Unless specified otherwise, the following simulations use a temperature set-point of $T_{load_sp} = 190\,^\circ$F, heat exchanger thermal mass $MCs = 0.65$, pipe diameter $d = 1.5$ in for the ram and bypass channels, and a valve time constant $\tau_v = 1.5$ s. The simulation time step is typically 0.1 s, and the heat-exchanger dimension is set to $N = 10$ in all the simulations.

A. Ram Air Channel Control

PI control is applied for the simulation of ram air channel control configuration shown in Fig. 1(a). The output of the ram air control, equivalent to the input to the valve, is given by the PI control law

$$u_{ram} = -\left(K_{P_{ram}} + \frac{K_{P_{ram}}}{T_{I_{ram}} S}\right) e_{temp} \quad (28)$$

where K_{Pram} and T_{Iram} are the PI-controller proportional gain and integral time constant, respectively.

The operating conditions in terms of temperatures, pressures, and flow rates, along with the tuned PI-control parameters for the ram-air controller, are listed in Table I.

TABLE I
Initial Values and Control Parameters for Ram Air Channel Control

K_{Pram}=0.2	T_{Iram}=100 sec	W_{bleed}=0.0183 lb/s
W_{ram}=0.0172 lb/s	T_{hi}=380 °F	T_{ci}=117.5 °F
P_{hin}= 45.11 psi	P_{amb}= 10.11psi	

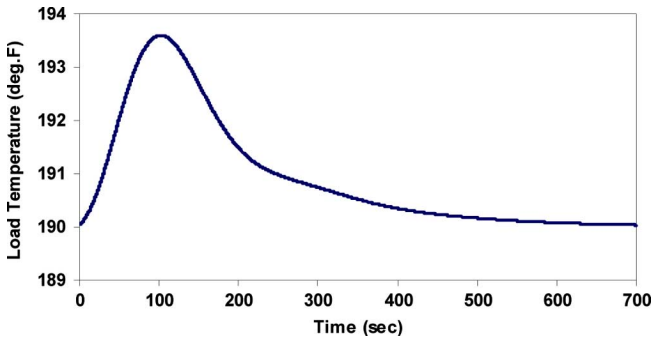

Fig. 5. Load temperature response to a $40\,^\circ$F step in T_{hi}.

To maintain the load temperature at a set-point, an increase in ram air flow rate is necessary to counteract the increased thermal energy carried by the bleed air. According to the simulation results, from the initial steady state value of $W_{ram} = 0.0172$ lb/s, the ram airflow rate increases to $W_{ram} = 0.0192$ lb/s for a $40\,^\circ$F increase in bleed temperature. As expected, the response time of this control scheme is rather large, as shown in Fig. 5, due to the sluggish heat exchanger dynamics.

This control scheme does have one major advantage: it does not waste any ram air. At steady state, the amount of ram air used is the lowest necessary value required for regulation; in other words, no overcooling of the heat exchanger hot-side stream takes place, unlike for cases with a hot-side bypass.

B. Bypass Channel Control

For simulation of the bypass channel control configuration shown in Fig. 1(b), the same temperature error e_{temp} signal drives the bypass controller, with a PI control law identical to (15). The operating conditions along with the PI-control parameters are listed in Table II.

An increase in bleed air inlet temperature will cause the heat exchanger hot-side outlet temperature T_{ho} to rise, and consequently a reduction in the bypass flow rate is required to restore the load temperature to its set-point. An important characteristic of this control scheme is its short response time, as confirmed

TABLE II
INITIAL VALUES CONTROL PARAMETERS FOR BYPASS CHANNEL CONTROL

$K_{Pbypass}$=5	$T_{Ibypass}$=25 sec	W_{bleed}=0.0183 lb/s
W_{ram}=0.273 lb/s	$W_{bleedmain}$=0.0133 lb/s	T_{ci}=117.5 °F
T_{hi}=380 °F	$W_{bleedbypass}$=0.005 lb/s	P_{hin}= 45.11 psi
P_{amb}= 10.11psi		

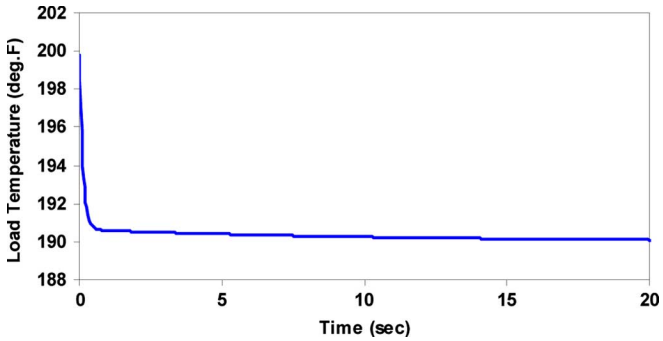

Fig. 6. Temperature response to a 40 °F step in T_{hi}.

TABLE III
INITIAL VALUES AND CONTROL PARAMETERS FOR RAM-AIR-PLUS-BYPASS CHANNEL CONTROL

$K_{Pbypass}$=6	$T_{Ibypass}$=15 sec	K_{Pram}=2
T_{Iram}=30 sec	W_{bleed}=0.0183 lb/s	P_{hin}= 45.11 psi
$W_{bleedmain}$= 0.0165 lb/s	W_{ram}= 0.0198 lb/s	T_{hi}=380 °F
$W_{bleedbypass}$=0.0018 lb/s	T_{ci}=117.5 °F	

by the load temperature response shown in Fig. 6. Disturbances in bleed air are also immediately felt, as indicated by the quite abrupt change in load temperature.

Without a control valve in the ram air channel, the ram air flow rate in this configuration is dictated by the heat exchanger cold-side pressure drop and is a function of the operating conditions (i.e., airspeed and atmospheric pressure). For this simulation, the ram airflow rate is $W_{ram} = 0.273\,\mathrm{lb/s}$. Note that this value is much larger than that in the ram air channel control case.

C. Ram-Air-Plus-Bypass Channel Control

For the proposed ram-air-plus-bypass channel control, both the PI and LQR control methods described in Section III were simulated. At initial conditions, the bypass valve opening is assumed to be at the desired set-point, such that the ratio of bypass to total bleed flow is low (10%). The corresponding steady-state values are listed in Table III.

By modulating both ram air and bypass channel flow rates, this control strategy is able to deliver efficient load temperature response while lowering the ram air usage penalty that is generally associated configurations employing a bleed air bypass. The simulation results shown in Fig. 7 agree with this hypothesis.

In the initial stages, actions of the bypass control valve quickly reduce the temperature error, with the remaining error slowly diminishing with time. The small variations in load temperature, made more visible in the inset plot of Fig. 7, are due to the slower-acting ram air channel controller modulating the ram air flow rate in order to slowly bring back the bypass valve opening to its set-point.

The dashed line in Fig. 7 is the load temperature response with LQR. With respect to a 40 °F step increase in bleed air inlet

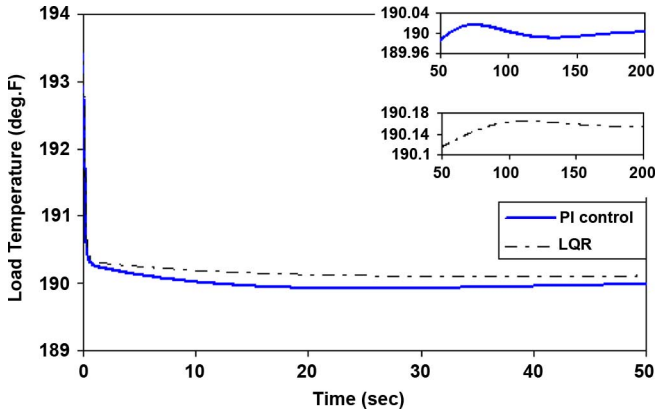

Fig. 7. Temperature response to a 40 °F step in T_{hi}.

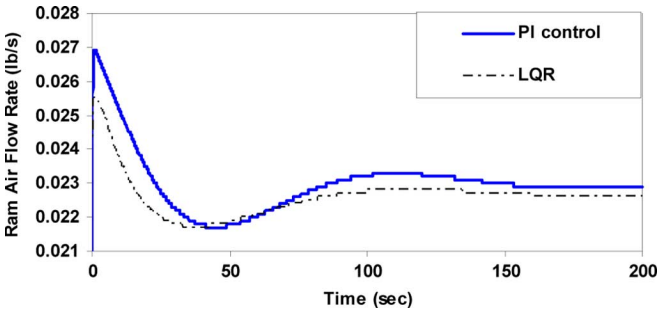

Fig. 8. Ram air flow rate response to a 40 °F step in T_{hi}.

TABLE IV
A COMPARISON OF RAM AIR USAGE FOR THE THREE CONTROL CONFIGURATIONS

	Initial (steady-state)	*Final* (steady-state)
Ram air channel control	0.0172 lb/s	0.0192 lb/s
Bypass channel control	0.273 lb/s	0.273 lb/s
Ram-air-plus-bypass channel control (PI)	0.0198 lb/s	0.0233 lb/s
Ram-air-plus-bypass channel control (LQR)	0.0198 lb/s	0.0222 lb/s

temperature at zero time, the load temperature is settled within 50 s, with a steady state error about 0.16 °F as shown in the inset plot of Fig. 7. With the weighting matrix Q and R tuned to optimize the temperature control error and the valve opening deviation, the optimal control gain matrix K_{lq} is determined as

$$K_{lq} = \begin{bmatrix} -6.04 & 0 \\ 9.51 & -15.37 \end{bmatrix}.$$

In terms of ram air usage, this configuration fares much better than the bypass channel control configuration. Only a slight increase in ram airflow rate, from the initial value of $W_{ram} = 0.0198\,\mathrm{lb/s}$ to a new value of $W_{ram} = 0.0233\,\mathrm{lb/s}$ (with PI control), and $W_{ram} = 0.0222\,\mathrm{lb/s}$ (with optimal control), when a 40 °F increase in bleed air temperature is simulated. And the dynamic response of ram air flow rate in Fig. 8 shows smaller overshoot and variation with LQR.

For comparison purposes, ram air usage for the three control configurations analyzed here are listed in Table IV below, in terms of initial and final steady-state values of ram air flow rate.

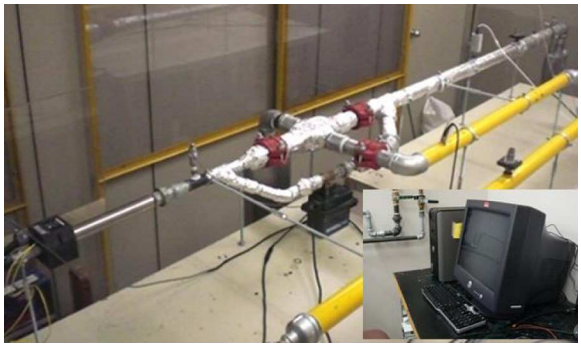

Fig. 9. Test rig for bleed air temperature control studies.

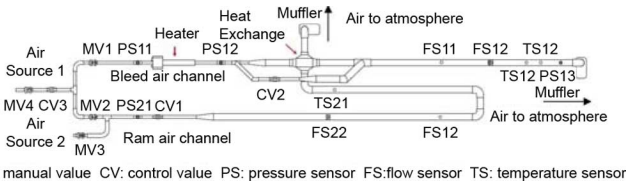

Fig. 10. Schematic layout of the test rig for bleed air temperature control studies.

V. Experimental Results

Experiments are conducted on a test rig in laboratory settings. The test rig is developed at our laboratory for the flow temperature control studies. Figs. 9 and 10 show the picture and schematic layout of the test rig, respectively. This test rig consists of a bleed air channel and a ram air channel. An in-line heater with temperature control is installed upstream the bleed air channel. A bypass channel is split from the bleed air channel over the heat exchanger. Electrical control valves are installed in the bypass channel and ram air channel to control the mass flow rate of each channel. A temperature sensor is installed at the outlet of bleed air channel to measure the load temperature. The test rig is also equipped with thermal mass flow sensors, pressure sensors, temperature sensors and manual valves, as shown in Fig. 10.

There are two air sources available for the experiments. The main air source is two parallel-connected high pressure tanks, each having a capacity of 51 300 in^3. The maximum pressure inside the tank is 100 psig, charged by a compressor. Although the compressor can continuously supply the compressed air to the tanks, the pressure of the air feeding to the test rig drops, depending upon the mass flow rate. To solve this problem, a control valve (CV3) is installed near the test rig. The inlet source air flow rate to the test rig is kept approximately constant by this control valve. The second air source is a separate tank charged by the same compressor, which supplies air for the ram air channel. The control valve (CV1) is installed to keep the ram air flow rate at the required value.

The experiments were conducted at a room temperature of about 70 °F and an atmospheric pressure of 14.7 psia. The in-line heater heats up the simulated bleed air to an inlet temeprature of 140 °F with the mass flow rate at 0.02 lb/s. The duration for each test is within 200 s.

There are two control inputs in the bleed air system. For the bleed air channel, the control input is bypass valve command signal. The control valve turns from "close" to "full open" while the command signal changes from 4 to 20 mA. For the ram air channel, because of the decreasing pressure of the air source, the control input is changed to ram air mass flow rate W_{ram}, instead of ram air valve opening ratio u_{ram}. The load temperature is measured by a temperature sensor. Since the delay of the temperature sensor is small compared to the response time of the load temperature in the tests, the sensor dynamics is not considered.

TABLE V
PI Control Gains for Different Control Configurations

	K_{Pram}	T_{Iram}	$K_{Pbypass}$	$T_{Ibypass}$
Ram air channel control	-0.003	100	/	/
Bypass channel control	/	/	1	20
Ram-air-plus-bypass channel control	0.001	100	1	20

TABLE VI
Operating Condition and Model Parameters

T_{hi}=140 ºF	T_{amb}=70 ºF	T_{load_sp}=86 ºF
W_{bleed}=0.02 lb/s	D_{bypass}=0.75 inch	D_{ram}=0.75 inch
$W_{bleedmain}$= 0.0182 lb/s	W_{ram}= 0.03 lb/s	H_h=0.024 Btu/s·ºR
$W_{bleedbypass}$=0.0018 lb/s	MC_s=0.7 Btu/ ºF	H_c=0.024 Btu/s·ºR
K_v=0.015708	τ_v=1.5 sec	N=10

The PI control gains were tuned to achieve the best achievable system response and listed in Table V. The optimal control gain matrix was calculated based on the operating condition and model parameters in Table VI as

$$K_{lq} = \begin{bmatrix} -0.979 & 0 \\ 0.0842 & -0.088 \end{bmatrix}.$$

The thermal mass MC_s is estimated by comparing the dynamic simulation and the actual response of the heat exchanger hot-side outlet temperature T_{ho}. With the change of flow temperature (3) and incremental of heat transfer (4), the overall heat transfer coefficients H_h and H_c are estimated as

$$H_h = H_c = \frac{W_{bleedmain} C_h \left(T_{ho} - T_{hi}\right) \ln\left(\frac{\Delta T_2}{\Delta T_1}\right)}{\Delta T_2 - \Delta T_1} \qquad (29)$$

where $\Delta T_1 = T_{ho} - T_{ci}$ and $\Delta T_2 = T_{hi} - T_{c0}$.

Figs. 11 and 12 show the time responses of load temperature and ram air flow rates, respectively, of different control strategies. A 2 °F step increase of the load temperature setting is applied at the zero time. The experimental results clearly show that the ram air channel control has the slowest response, taking about 200 s to reach the steady-state. But the usage of ram air flow is low, only changes from 0.019 to 0.015 lb/s. For bypass channel control, it has the fastest time response, but the corresponding ram air flow rate is significantly higher, which is around 0.04 lb/s. For ram-air-plus-bypass channel control, the ram air mass flow rate changes from 0.03 to 0.028 lb/s. Compared to bypass control, this configuration shows significant saving of ram air. And the load temperature response is much faster than that of ram air channel control.

In Fig. 13, compared with PI control, the load temperature of the ram-air-plus-bypass channel control configuration under LQR shows a similar dynamic response.

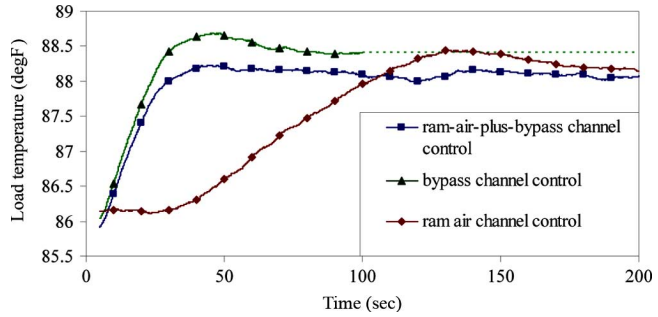

Fig. 11. Load temperature response to a 2 °F step in T_{load_sp} under PI control.

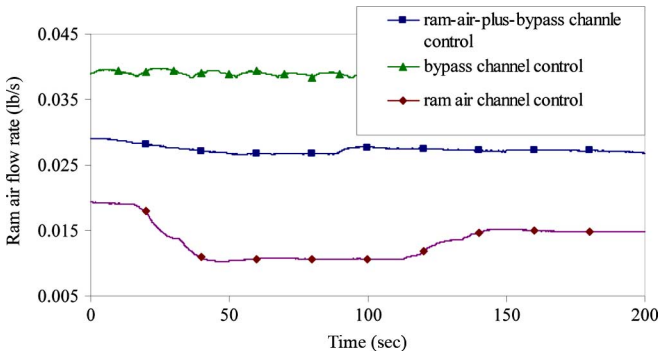

Fig. 12. Ram air flow rate response to a 2 °F step in T_{load_sp} under PI control.

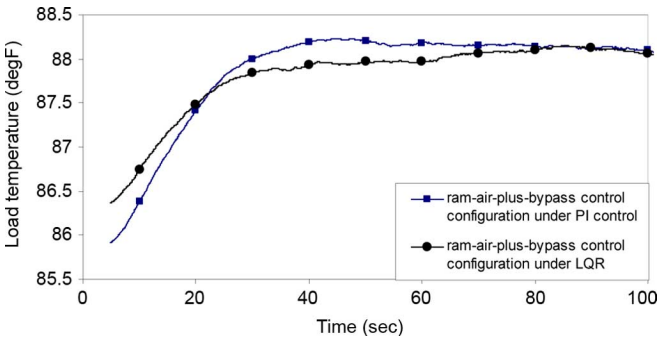

Fig. 13. Load temperature response of ram-air-plus-bypass channel control to a 2 °F step in T_{load_sp}.

The steady-state error and small swing of the system response can be seen from the experimental results. It may be caused by many factors. First, some errors are introduced by the linearization of system model, which is the based on the first order Taylor Expansion. System model is not exactly the same the real system because of the assumptions made in Section II. Some system parameters may not be identified accurately. The temperature errors and small variation may also be caused by sensor measurement error, heat loss through the metal pipes, and unmodeled dynamics of the control valves.

VI. Conclusion

Although the ram air control scheme minimizes ram air usage, its response time is large, making this strategy undesirable in applications where fast response is of importance. On the other hand, manipulating the bleed air bypass channel flow rate only drastically reduces the response time at the expense of using significantly more ram air than the former control strategy.

The proposed ram air and bypass control strategy effectively combines desirable features of the above two methods, and is an improvement over the former, in terms of satisfying both the requirements of fast response speed and ram air reduction. A lower bypass flow rate leads to more efficient ram air usage, since it requires less overcooling of the main bleed channel. Adding the bypass valve opening as a secondary controlled variable gives this method a way of maintaining this lowered ram air usage. By regulating the bypass valve opening at its predefined set-point, this control strategy guarantees that some bypass flow will always be present, thus ensuring the efficient response behavior characteristic to configurations with a bypass.

Substantially less ram air is used by the ram-air-plus-bypass control strategy than for the bypass channel control configuration, as demonstrated in the simulations and experiments; although employing a bleed air bypass means that more ram air is used than for the ram air control scheme. However, by setting the bypass valve opening set-point at a low value, this difference can be kept reasonably small. The advantages of significantly reducing the response time in this case outweigh the slight increase in ram air usage.

References

[1] B. Burkett, M. Metrovic, D. Sweet, G. Botura, D. Burner, M. Layland, and K. Brown, "Development and test results on a high efficientily ice protection system," presented at the 44th AIAA Aerosp. Sci. Meet. Exhibit, Reno, NV, 2006, AIAA-2006-863.

[2] T. Ensign and J. Gallman, "Energy optimized equipment systems for general aviation jets," presented at the 44th AIAA Aerospace Sciences Meeting and Exhibit, Reno, NV, 2006, AIAA-2006-228.

[3] R. Gandolfi, L. Pellegrini, G. Silva, and S. Oliveira, "Exergy analysis applied to a complete flight mission of commercial aircraft," presented at the 46th AIAA Aerospace Sciences Meeting and Exhibit, Reno, NV, 2008, AIAA-2008-153.

[4] G. Liu, G. Bao, C. Lam, and J. Jiang, "A master-slave approach to aircraft engine bleed flow sharing control," *IEEE Trans. Control Syst. Technol.*, vol. 13, no. 6, pp. 1100–1106, Nov. 2005.

[5] W. M. Kays and A. L. London, *Compact Heat Exchangers*. New York: McGraw-Hill, 1964.

[6] T. Katayama, T. Itoh, M. Ogawa, and H. Yamamoto, "Optimal tracking control of a heat exchanger with change in load condition," in *Proc. 29th Conf. Dec. Control*, 1990, vol. 3, pp. 1584–1589.

[7] V. P. Paruchuri and R. R. Rhinehart, "Experimental demonstration of nonlinear model-based-control of a heat exchanger," in *Proc. Amer. Control Conf.*, 1994, vol. 3, pp. 3533–3537.

[8] M. Komareji, J. Stoustrup, H. Rasmussen, N. Bidstrup, P. Svendsen, and F. Nielsen, "Optimal set-point synthesis in HVAC systems," in *Proc. Amer. Control Conf.*, 2007, pp. 5076–5081.

[9] M. A. Rotea and J. L. Marchetti, "Integral control of heat exchanger plus bypass systems," in *Proc. IEEE Int. Conf. Control Appl.*, 1997, pp. 151–156.

[10] S. Forrest, M. Johnson, and M. Grimble, "LQG self-tuning control of super-heated steam temperature in power generation," in *Proc. IEEE Conf. Control Appl.*, 1993, vol. 2, pp. 805–810.

[11] M. Orzylowski, T. Kaluzniacki, Z. Rudolf, and G. Nowicki, "Precise temperature control for measurement purposes," in *Proc. Instrumentation Meas. Technol. Conf.*, 1999, vol. 1, pp. 16–21.

[12] T. S. Pedersn, T. Hansen, and M. Hangstrup, "Process-optimizing multivariable control of a boiler system," in *Proc. UKACC Int. Conf. Control*, 1996, vol. 2, pp. 787–792.

[13] P. Hodal and G. Liu, "Bleed air temperature regulation system: Modeling, control, and simulation," in *Proc. IEEE Int. Conf. Control Appl.*, 2005, pp. 1003–1008.

[14] F. P. Incropera and D. P. Dewitt, *Fundamentals of Heat and Mass Transfer*. New York: Wiley, 1996.

[15] R. K. Rajamani and J. A. Herbst, "Optimal control of a ball mill grinding circuit. II. Feedback and optimal control," *Chem. Eng. Sci.*, vol. 1, pp. 871–879, 1991.